



CHALMERS
UNIVERSITY OF TECHNOLOGY

Effect of Si addition on Curie temperature and thermal expansion coefficient of

Downloaded from: <https://research.chalmers.se>, 2024-11-19 08:21 UTC





Citation for the original published paper (version of record):

Wang, Z., Yang, T., Wu, D. et al (2024). Effect of Si addition on Curie temperature and thermal expansion coefficient of (Fe^{71.2}B²⁴Y^{4.8})₉₆Nb₄ Invar bulk metallic glasses. *Journal of Applied Physics*, 136(4). <http://dx.doi.org/10.1063/5.0211847>

N.B. When citing this work, cite the original published paper.

RESEARCH ARTICLE | JULY 30 2024

Effect of Si addition on Curie temperature and thermal expansion coefficient of $(\text{Fe}_{71.2}\text{B}_{24}\text{Y}_{4.8})\text{Nb}_4$ Invar bulk metallic glasses

Z. R. Wang ; T. Yang; D. Wu; C. M. Wang; H. Guo; Q. Hu  ; S. Guo 

 Check for updates

J. Appl. Phys. 136, 045110 (2024)

<https://doi.org/10.1063/5.0211847>





Instruments for Advanced Science

■ Knowledge
■ Experience ■ Expertise

[Click to view our product catalogue](#)

Contact Hiden Analytical for further details:
www.HidenAnalytical.com
info@hiden.co.uk

Gas Analysis

- ▶ dynamic measurement of reaction gas streams
- ▶ catalysis and thermal analysis
- ▶ molecular beam studies
- ▶ dissolved species probes
- ▶ fermentation, environmental and ecological studies

Surface Science

- ▶ UHV-TPD
- ▶ SIMS
- ▶ end point detection in ion beam etch
- ▶ elemental imaging - surface mapping

Plasma Diagnostics

- ▶ plasma source characterization
- ▶ etch and deposition process reaction kinetic studies
- ▶ analysis of neutral and radical species

Vacuum Analysis

- ▶ partial pressure measurement and control of process gases
- ▶ reactive sputter process control
- ▶ vacuum diagnostics
- ▶ vacuum coating process monitoring

Effect of Si addition on Curie temperature and thermal expansion coefficient of $(\text{Fe}_{71.2}\text{B}_{24}\text{Y}_{4.8})_{96}\text{Nb}_4$ Invar bulk metallic glasses

Cite as: J. Appl. Phys. 136, 045110 (2024); doi: 10.1063/5.0211847

Submitted: 2 April 2024 · Accepted: 12 July 2024 ·

Published Online: 30 July 2024



Z. R. Wang,^{1,2}  T. Yang,² D. Wu,¹ C. M. Wang,¹ H. Guo,¹ Q. Hu,^{1,a)}  and S. Guo³ 

AFFILIATIONS

¹Institute of Applied Physics, Jiangxi Academy of Sciences, Nanchang 330096, China

²Key Laboratory for Microstructural Control of Metallic Materials of Jiangxi Province, Nanchang Hangkong University, Nanchang 330063, People's Republic of China

³Industrial and Materials Science, Chalmers University of Technology, SE-41296 Göteborg, Sweden

^{a)}Author to whom correspondence should be addressed: q-fei618@qq.com

ABSTRACT

The ultra-low thermal expansion coefficient α makes the Fe-Ni Invar alloys useful in various applications. Their low strength and low Curie temperature T_c are, however, limiting factors. Interestingly, some Fe-based bulk metallic glasses (BMGs), with inherent high strength, exhibit the clear Invar effect. In particular, the $(\text{Fe}_{71.2}\text{B}_{24}\text{Y}_{4.8})_{96}\text{Nb}_4$ BMG has the lowest α among Fe-based BMGs, but it unfortunately also has the lowest T_c . In this work, silicon was added into this alloy with the aim to elevate T_c while maintaining a low α . It was found that when silicon partially substituted boron, T_c did not increase significantly but α did, which is not ideal. On the other hand, when silicon partially substituted yttrium and niobium and especially niobium, T_c increased significantly while α did not, which is close to the ideal scenario. When 3% of niobium was substituted by silicon, T_c reached the maximum value of 296 °C while α remained a low value of $7.4 \times 10^{-6}/^\circ\text{C}$. Comparing to the Fe-Ni Invar alloy, although this BMG has an inferior α , it has much higher T_c (+115 °C) and strength (~9 times), presenting a potential for application as a new Invar material with moderate (low) thermal expansion, high operating temperature, and high strength.

© 2024 Author(s). All article content, except where otherwise noted, is licensed under a Creative Commons Attribution (CC BY) license (<https://creativecommons.org/licenses/by/4.0/>). <https://doi.org/10.1063/5.0211847>

I. INTRODUCTION

The Invar effect refers to the anomalous low thermal expansion behavior occurring in some weak magnets,¹ below the magnetic transition point known as the Curie temperature, T_c . The room-temperature thermal expansion coefficient, α , of $\text{Fe}_{64}\text{Ni}_{36}$, i.e., the Invar alloy, is only $1.2 \times 10^{-6}/^\circ\text{C}$,²⁻⁵ an order of magnitude lower than that of Fe and Ni. Owing to the low thermal expansion characteristic, the Invar alloy has a wide range of applications in precision measuring instruments, long distance power cable, satellite positioning systems, liquefied natural gas (LNG) carrier, etc.⁶ The Invar alloy however, with the face center cubic (FCC) structure, has a limited strength lower than 1000 MPa.^{7,8} In addition, the limited operating temperature range for the Invar effect to be effective is another concern. For example, the ultra-low α of the Invar alloy is only effective below 80 °C; above 80 °C, α begins to

increase but still in the order of $10^{-6}/^\circ\text{C}$; however, above T_c and in this case 200 °C, the low thermal expansion characteristic completely disappears. The low strength and low T_c of the existing Invar-like alloys, i.e., alloys with ultra-low thermal expansion coefficient, are challenging issues to be tackled. Therefore, it is rewarding to seek other alloys with low thermal expansion, high strength, and high operating temperature (higher T_c).

Interestingly, besides the fcc-structured Fe-Ni alloys, many Fe-based bulk metallic glasses (BMGs) also exhibit the typical Invar effect.⁹ Owing to their disordered structure, these alloys have a strength as high as 4000 MPa.¹⁰⁻¹² Among the Fe-based Invar BMGs, $(\text{Fe}_{71.2}\text{B}_{24}\text{Y}_{4.8})_{96}\text{Nb}_4$ has the strongest Invar effect, i.e., the lowest α of $5.5 \times 10^{-6}/^\circ\text{C}$, but unfortunately also the lowest T_c of 178 °C.^{9,13} On the other hand, $(\text{Fe}_{75}\text{B}_{20}\text{Si}_5)_{96}\text{Nb}_4$ with a much higher T_c of 312 °C also exhibits a clear Invar effect with α of

11 September 2024, 07:45:28

$7.4 \times 10^{-6}/^{\circ}\text{C}$.⁹ These two alloys have rather close compositions, with mainly silicon replacing yttrium in the latter. Inspired by that, here we proposed to add silicon into $(\text{Fe}_{71.2}\text{B}_{24}\text{Y}_{4.8})_{96}\text{Nb}_4$ or to add yttrium into $(\text{Fe}_{75}\text{B}_{20}\text{Si}_5)_{96}\text{Nb}_4$ to experiments whether a more balanced α and T_c could be achieved by the alloying effect. The first strategy was employed here in this work, mainly because $(\text{Fe}_{71.2}\text{B}_{24}\text{Y}_{4.8})_{96}\text{Nb}_4$ has a much better glass-forming ability and thus a broader glass-forming compositional range could be expected when adjusting the alloy compositions.¹⁴ In total, 16 new alloys, were developed by adding silicon into the base $(\text{Fe}_{71.2}\text{B}_{24}\text{Y}_{4.8})_{96}\text{Nb}_4$ alloy, to partially substitute boron, yttrium, or niobium, but not iron, because both the Invar effect and the Curie transition originate from the ferromagnetic element,³ iron in this case. Results from this work are expected to facilitate future developments of novel Fe-based Invar BMGs with low thermal expansion and high operating temperatures.

II. EXPERIMENTAL DETAILS

The master alloys were prepared by arc melting in a Ti-gettered high-purity argon atmosphere. First, pure Fe (99.99%), Nb (99.99%) and Si (99.9999%) were mixed and melted three times in the copper crucible. Pure Y (99.99%) and high-purity $\text{Fe}_{78}\text{B}_{22}$ (99.99%) binary alloys were then added and the mixture was melted four times. BMG rods with a diameter of 1 mm and a length of 50 mm were prepared by copper mold casting. The amorphous state was verified by x-ray diffraction (XRD Bruker D8 Advance, 40 KV \times 200 mA). The thermal expansion behavior was evaluated by the dilatometer (NETZSCH DIL 402C) using samples with a diameter of 1 mm and a length of 20 mm. The applied push load was 0.3 N and the heating rate was $5^{\circ}\text{C}/\text{min}$. The glass transition temperature T_g and crystallization temperature T_x were measured by the differential scanning calorimeter (NETZSCH DSC 404F3) with a heating rate of $5^{\circ}\text{C}/\text{min}$. The thermomagnetic behavior was measured by the vibrating sample magnetometer (VSM-HH15) under 1.5 T of external magnetic field, with a heating rate of $5^{\circ}\text{C}/\text{min}$. The quasistatic-compression tests were carried out on the BMG rod with a dimension of $\phi 1 \text{ mm} \times 2 \text{ mm}$ using a universal testing machine (MTS, CMT5205) with an initial strain rate of $1 \times 10^{-4}/\text{s}$. The commercial Invar alloy ($\text{Fe}_{64}\text{Ni}_{36}$, wt.%) rod and cold-drawn SUS 304 rod were also compression tested with the same initial strain rate for comparison. Rod samples with a larger dimension of $\phi 5 \text{ mm} \times 2 \text{ mm}$ were employed for an accurate determination of the yield strength, since these two FCC alloys have a much poorer strength than the Fe-based BMG. The compression tests for the BMG ended when the sample fractured, with the data presenting as the engineering stress and strain, while the tests for the Invar alloy and SUS 304 ended when the load reached 50 KN, with the data presenting as the true stress and strain.

III. RESULTS

Silicon was added into the base $(\text{Fe}_{71.2}\text{B}_{24}\text{Y}_{4.8})_{96}\text{Nb}_4$ alloy, i.e., $\text{Fe}_{68.352}\text{B}_{23.04}\text{Y}_{4.608}\text{Nb}_4$. In total, 16 new alloys were designed, including $\text{Fe}_{68.352}\text{B}_{23.04-x}\text{Y}_{4.608}\text{Nb}_4\text{Si}_x$ ($x = 0.25, 0.5, 0.75, 1, 2, 3, 4.3, 4.8, 8, 9$), $\text{Fe}_{68.352}\text{B}_{23.04}\text{Y}_{4.608-y}\text{Nb}_4\text{Si}_y$ ($y = 1, 2, 3$) and $\text{Fe}_{68.352}\text{B}_{23.04}\text{Y}_{4.608}\text{Nb}_{4-z}\text{Si}_z$ ($z = 1, 2, 3$). As shown in the XRD patterns given in Fig. 1, all alloys with a diameter of 1 mm had a fully

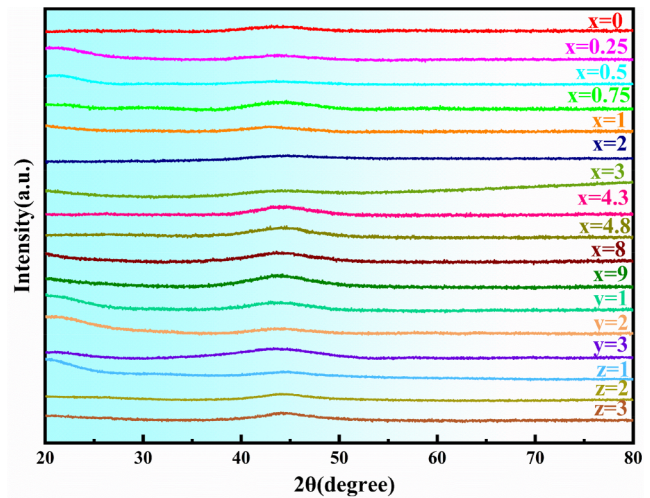


FIG. 1. XRD patterns of $\text{Fe}_{68.352}\text{B}_{23.04-x}\text{Y}_{4.608}\text{Nb}_4\text{Si}_x$, $\text{Fe}_{68.352}\text{B}_{23.04}\text{Y}_{4.608-y}\text{Nb}_4\text{Si}_y$, and $\text{Fe}_{68.352}\text{B}_{23.04}\text{Y}_{4.608}\text{Nb}_{4-z}\text{Si}_z$ BMGs with a diameter of 1 mm.

amorphous structure. Indeed, BMGs with a diameter of at least 2 mm could be formed in most of these alloys. However, when the silicon content was higher than 4%, fully amorphous samples could only be made with a diameter of 1 mm. Therefore, all samples with a diameter of 1 mm were used for consistency.

Figure 2 shows that all alloys exhibited the typical Invar effect, manifested as a low thermal expansion in the low temperature region and a higher thermal expansion in the high temperature region. The transition temperature is the Curie temperature, $T_{c-\text{DIL}}$, determined by the dilatometer (DIL) test.^{9,13,15} The ferromagnetic transformation is abrupt in the DIL trace, and the alloys are ferromagnetic below $T_{c-\text{DIL}}$ and paramagnetic above $T_{c-\text{DIL}}$. In the thermomagnetic (TM) test done under an applied magnetic field, as shown in Fig. 3, the ferromagnetic transformation is a prolonged process. The magnetization intensity decreased continuously with the increase of temperature. The ending temperature of the prolonged ferromagnetic transition is also the Curie temperature, $T_{c-\text{TM}}$. $T_{c-\text{TM}}$ was very close to $T_{c-\text{DIL}}$, and as an example this could be clearly seen for the base $(\text{Fe}_{71.2}\text{B}_{24}\text{Y}_{4.8})_{96}\text{Nb}_4$ alloy, as shown in Fig. 4. Figure 5 further shows that the Curie temperatures determined by these two methods were rather close. $T_{c-\text{DIL}}$ is, therefore, simplified to T_c in the following discussion.

From Fig. 2, it is clear that the silicon addition increased both T_c and α , no matter which element was substituted. The alloying effect on T_c and α , however, was quite different. When silicon partially substituted boron, both T_c and α increased with the increase of silicon content, as indicated in Fig. 6. The increase of α , i.e., the weakening of the Invar effect, can be explained using the concept of effective valence electron number,^{16,17} N_{eff} , which is defined as

$$N_{\text{eff}} = \left(\sum_i x_i N_{\text{tm}} / \sum_i x_i + \sum_i y_i N_{\text{ml}} \right) / \left(1 - \sum_i y_i \right), \quad (1)$$

where x_i is the content of transition metal elements containing 3d valence electrons, y_i is the content of metalloid elements, N_{tm} is the

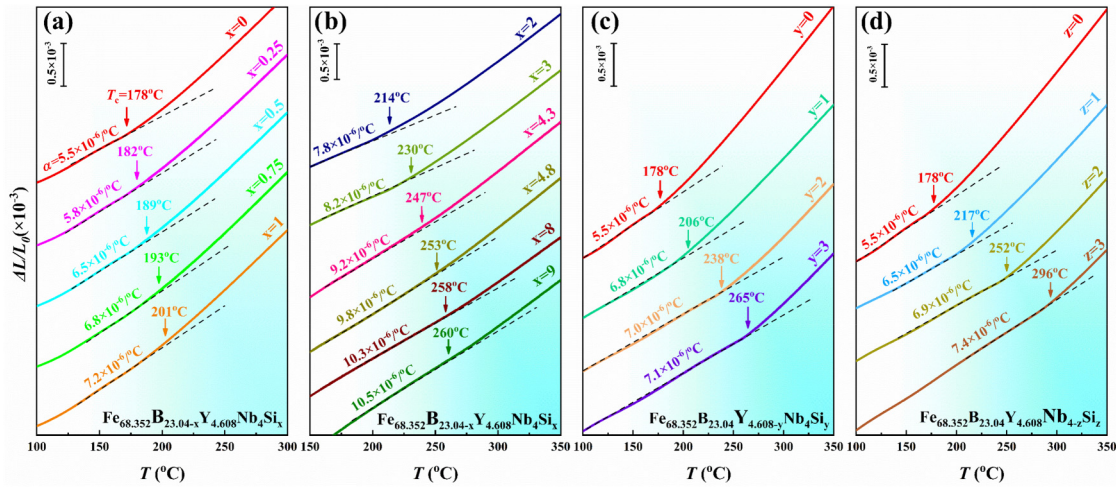


FIG. 2. DIL traces of (a) and (b) $\text{Fe}_{68.352}\text{B}_{23.04-x}\text{Y}_{4.608}\text{Nb}_4\text{Si}_x$, (c) $\text{Fe}_{68.352}\text{B}_{23.04}\text{Y}_{4.608-y}\text{Nb}_4\text{Si}_y$, and (d) $\text{Fe}_{68.352}\text{B}_{23.04}\text{Y}_{4.608}\text{Nb}_{4-z}\text{Si}_z$ BMGs.

number of $3d + 4s$ valence electrons of the transition metal elements, and N_{ml} is the number of donor electrons per metalloidal atom, viz., 1, 2, 3 for B, Si, P, respectively. It was found that Fe-based BMGs with N_{eff} near 8.2 have the most intense Invar effect;^{16–19} any deviation from N_{eff} of 8.2, whether positive or negative, would deteriorate the Invar effect, and a larger deviation would result in a more weakened Invar effect. N_{eff} of the base ($\text{Fe}_{71.2}\text{B}_{24}\text{Y}_{4.8}$) Nb_4 alloy is 8.3, which is the smallest among newly developed Fe-based BMGs but still positively deviating from 8.2. N_{eff} further increased when boron, which donates one electron, was substituted by silicon that donates two electrons. Therefore, the Invar effect weakened and α increased with the increasing silicon content. On the other hand, when the total content of (B + Si) was

constant and lower than 25%, the increase of silicon, which has a larger atomic radius than boron, could widen the Fe–Fe pair distance.²⁰ According to Bethe’s curve, a larger Fe–Fe pair distance would result in elevated T_c .^{9,21} Indeed, α increased since the Invar effect is closely related to the Fe–Fe pairs with a small distance.^{22,23}

T_c of the base $\text{Fe}_{68.352}\text{B}_{23.04}\text{Y}_{4.608}\text{Nb}_4$ alloy is 178 °C, which is significantly lower than T_c of 374 ~ 487 °C of the binary $\text{Fe}_{100-x}\text{B}_x$ ($x = 20\text{--}28$) amorphous alloys.^{24–26} Apparently, the unusually low T_c in the base $\text{Fe}_{68.352}\text{B}_{23.04}\text{Y}_{4.608}\text{Nb}_4$ alloy is attributed to the doping of niobium and yttrium. As shown in Figs. 2(c) and 3(c), when adding 1% of silicon to substitute niobium and yttrium, T_c increased by 39 and 28 °C, respectively; when adding 3% of silicon to substitute niobium and yttrium, T_c increased by 118 and 87 °C,

11 September 2024, 07:45:28

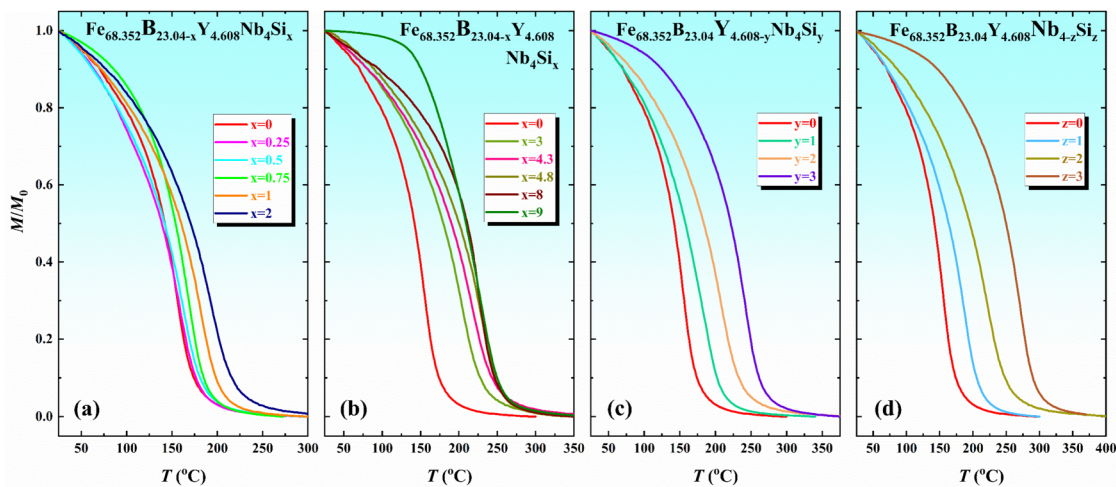


FIG. 3. Thermomagnetic traces of (a) and (b) $\text{Fe}_{68.352}\text{B}_{23.04-x}\text{Y}_{4.608}\text{Nb}_4\text{Si}_x$, (c) $\text{Fe}_{68.352}\text{B}_{23.04}\text{Y}_{4.608-y}\text{Nb}_4\text{Si}_y$, and (d) $\text{Fe}_{68.352}\text{B}_{23.04}\text{Y}_{4.608}\text{Nb}_{4-z}\text{Si}_z$ BMGs.

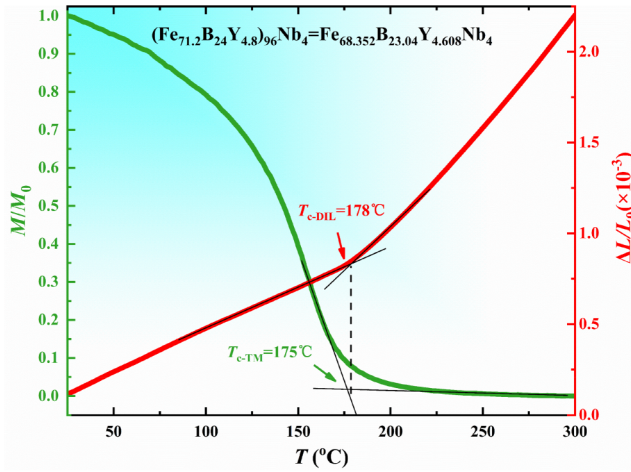


FIG. 4. Determination of the Curie temperature from the DIL and thermomagnetic traces, exemplified by the base $(\text{Fe}_{71.2}\text{B}_{24}\text{Y}_{4.8})_{96}\text{Nb}_4$ alloy.

respectively. Apparently, niobium has a more significant effect to elevate T_c than yttrium. Similar phenomena were also reported in the Fe-B-Nb and Fe-B-Y amorphous alloys,²⁷ as shown in Fig. 7. T_c increased by $\sim 25^\circ\text{C}$ in $\text{Fe}_{86-x}\text{B}_{14}\text{Nb}_x$ and $\text{Fe}_{88}\text{B}_{12-x}\text{Nb}_x$ amorphous alloys with the decrease of per 1% of niobium, but only increased by $\sim 14^\circ\text{C}$ in $\text{Fe}_{83}\text{B}_{17-x}\text{Y}_x$ amorphous alloys with the decrease of per 1% of yttrium.²⁷ The above phenomena could be attributed to the much lower T_c of the Fe-Nb binary compounds ($-223 \sim -73^\circ\text{C}$)²⁸ than that of the Fe-Y ($47 \sim 84.4^\circ\text{C}$)^{29,30} binary compounds. The Fe-Y and Fe-Nb pairs form short-range

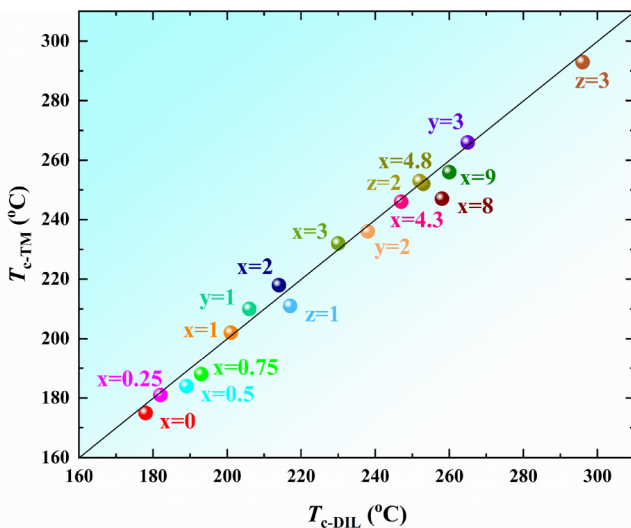


FIG. 5. Correlation between $T_{c\text{-TM}}$ and $T_{c\text{-DIL}}$ for Fe-based Invar BMGs.

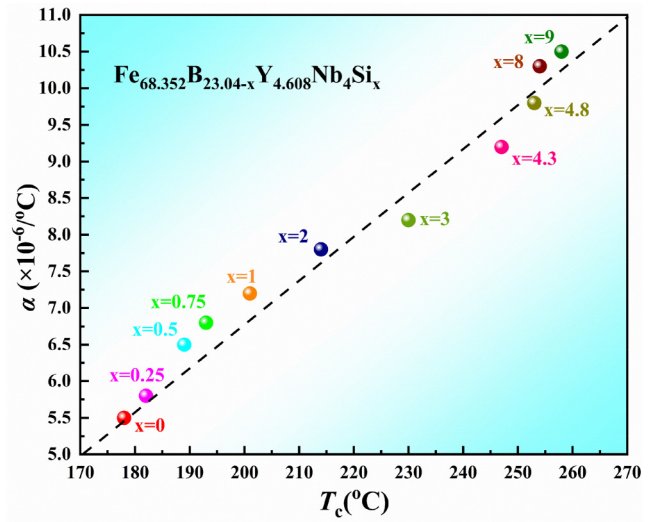


FIG. 6. Relationship between α and T_c when silicon partially substituted boron.

order in the base $\text{Fe}_{68.352}\text{B}_{23.04}\text{Y}_{4.608}\text{Nb}_4$ alloy (amorphous), which were verified by *in situ* synchrotron-based high-energy x-ray diffraction,^{22,23} and they very likely inherit the characteristic of Fe-Y and Fe-Nb from binary compounds in the crystalline form. T_c of amorphous alloys thus increases more quickly with the decrease of niobium than the decrease of yttrium, regardless of the substitution of niobium and yttrium by silicon or iron, as shown by the Fe-B-Y-Nb-Si, Fe-B-Y, and Fe-B-Nb alloys in Fig. 7.

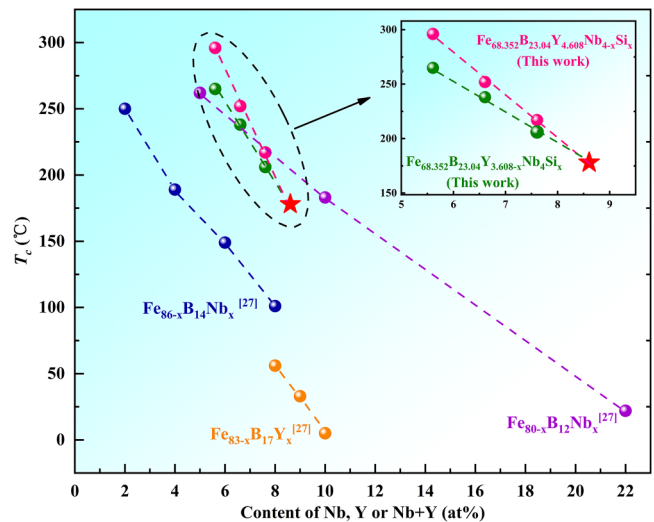


FIG. 7. Correlation between T_c and the content of Nb, Y, or Nb + Y of Fe-based amorphous alloys.

11 September 2024, 07:45:28

The Invar effect is a characteristic of weak magnets.^{1,3,5,9} When the compositional adjustment brings in an elevation of T_c , it also results in an increase of α , as indicated in this work and all previous reports.^{9,19,22,23,26,31-35} The difficulty is how to increase T_c quickly and meanwhile to slow down the increase of α . As shown in Fig. 8, when adding silicon to substitute boron, T_c did not increase so much but α did, which is not ideal. On the contrary, when silicon was added to substitute yttrium or niobium, T_c increased significantly while α did not increase so much, which is desirable. When 3% of niobium was substituted by silicon, i.e., $\text{Fe}_{68.352}\text{B}_{23.04}\text{Y}_{4.608}\text{Nb}_1\text{Si}_3$, T_c reached the maximum value of 296 °C and α only increased 34% when comparing to the base alloy, thus achieving a decent balance between low thermal expansion and high operating temperature.

As shown by the DSC trace in Fig. 9, the $\text{Fe}_{68.352}\text{B}_{23.04}\text{Y}_{4.608}\text{Nb}_1\text{Si}_3$ BMG has a high crystallization temperature T_x of 648 °C and thus good thermal stability. Before crystallization, there is a prolonged endothermic glass transition process, which begins at the onset temperature T_{g-on} of 559 °C and ends at T_{g-end} of 580 °C. On the other hand, α increases with the glass transition due to the free volume generation and then drops quickly due to softening.³⁶ The α peak temperature of 582 °C is very close to T_{g-end} , since at this point the alloy is completely transformed from the solid state to the soft super-cooled liquid state. When the temperature further elevates to T_x , the alloy begins to shrink and releases the heat very fast, manifested as the synchronous sharp peaks of the DSC and α traces.

The long-range atomic rearrangement during crystallization brings a great change in the distribution of Fe-Fe nearest

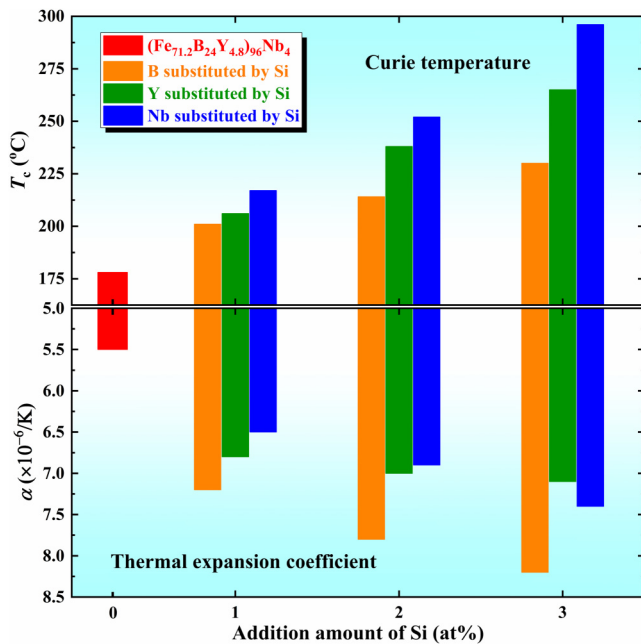


FIG. 8. Effect of Si addition on α and T_c of Fe-based Invar BMGs.

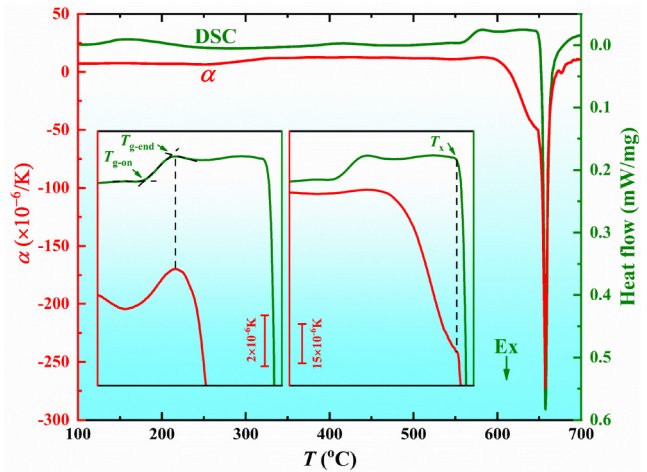


FIG. 9. DSC and α traces of $\text{Fe}_{68.352}\text{B}_{23.04}\text{Y}_{4.608}\text{Nb}_1\text{Si}_3$ BMG.

neighbors' distance, and thus deteriorates the Invar effect.^{9,37} As shown in Fig. 10(a), the sample is first heated above T_x to 720 °C, cooled down, and then reheated. The α trace has a step-type transition,⁹ which signals the Invar effect, in the first heating process. The steepest point of the step-type α transition is T_c , corresponding to the inflection point in the DIL trace. In the cooling and reheating processes, the step-type α transition at 300 °C disappears, indicating the vanishing of the Invar effect. On the other hand, as shown in Fig. 10(b), after first heating to 600 °C ($T_{g-end} < 600 \text{ °C} < T_x$), the Invar effect almost remains the same, in spite of a slightly increased T_c , in the following cooling and reheating processes. Therefore, as long as crystallization does not occur, the Invar effect stays.

Note that the cooling α trace of Fig. 10(a), and the first heating and cooling α traces of Fig. 10(b), are not fully displayed,

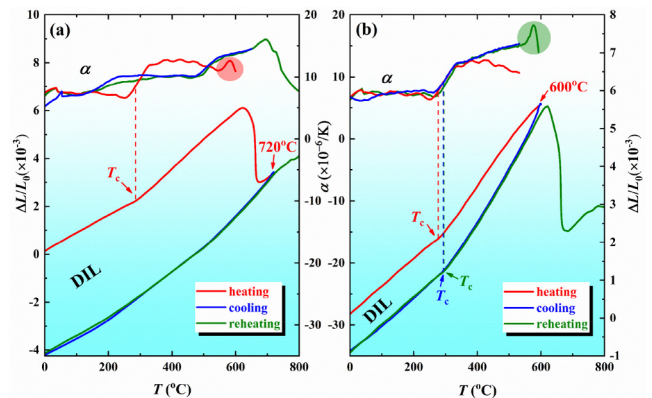


FIG. 10. DIL and α traces of the $\text{Fe}_{68.352}\text{B}_{23.04}\text{Y}_{4.608}\text{Nb}_1\text{Si}_3$ BMGs first heated to (a) 720 °C and (b) 600 °C, cooled down, and then reheated.

11 September 2024, 07:45:28

due to the inaccurate values when the program switches from heating to cooling. Similarly, the first heating α trace of Fig. 10(a) and the reheating α trace of Fig. 10(b) are also not fully displayed, due to the α value runout in softening and crystallization. As indicated by the shaded circles, the α peak shown in Fig. 10(b) is higher than that shown in Fig. 10(a). This phenomenon is attributed to more free volume generation during glass transition for the deeply annealed sample, i.e., the sample first heated to 600 °C that is in the super-cooled liquid region, and then cooled down with a slow heating rate of 5 K/min. According to the free volume theory,^{38,39} the less free volume annihilation in the structural relaxation, the more free volume generation in the glass transition, and vice versa. This regularity is universally applied in several scenarios that cause the free volume difference, including cooling rate in sample preparation,^{36,40,41} annealing temperature or annealing time,^{42,43} heating rate used in measurements,^{36,44} etc.

Figure 11 compares the thermal expansion behavior and mechanical property of three kinds of alloys. Admittedly, α of the BMG is inferior than the Fe–Ni Invar alloy, but it is much lower than that of the commonly used SUS304 alloy, indicating a considerable low expansion characteristic. It is worth noting that, as shown by the DIL traces of Fig. 11(a), the Fe–Ni alloy has a much gradual transition than the BMG. Technically, this is probable because of the much larger difference in the α value of the ferromagnetic and paramagnetic states, as marked in Fig. 11(a), of the Fe–Ni alloy than that of BMG. In physics, this phenomenon shows the quite different local atomic magnetic structure between the FCC alloy and amorphous Fe-based alloy, which is beyond the topic of this work but deserves further in-depth studies. On the other hand, more importantly, the BMG has two significant advantages over the Fe–Ni Invar alloy, one being T_c is 115 °C higher, and the other being the yield strength, σ_y , is about nine times higher, as shown in Fig. 11(b). Three kinds of alloys exhibit quite different mechanical properties. The BMG is very strong but completely brittle due to the disorder structure and strong Fe–B bonding.⁴⁵ Both SUS304 and the Fe–Ni Invar alloy have an FCC

structure and thus a good plasticity but simultaneously a much worse strength than the BMG. Comparatively, the commercial Fe–Ni alloy is even softer, and more importantly its work hardening ability is much weaker than that of SUS304. The Invar alloy containing carbide-forming elements can be strengthened to 1166 MPa by cold drawing,⁸ at the cost of a larger α of $4.9 \times 10^{-6}/\text{K}$. Even so, the strength cannot be comparable to the BMG. However, the $\text{Fe}_{68.352}\text{B}_{23.04}\text{Y}_{4.608}\text{Nb}_1\text{Si}_3$ BMG has also an obvious shortcoming, showing a poor GFA with the critical diameter of 1 mm. Nevertheless, this BMG still has potential in the application scenarios that require a high strength, high operating temperature, and a small thickness, like the thermal bimetal plate.

IV. CONCLUSION

In conclusion, it was found that the Curie temperature, T_c , determined by thermal expansion tests was close to the ending temperature of the ferromagnetic transition determined by thermomagnetic tests. Yttrium and niobium, especially the latter, were the main reason of the low T_c of $(\text{Fe}_{71.2}\text{B}_{24}\text{Y}_{4.8})_{96}\text{Nb}_4$. When silicon partially substituted boron, T_c did not increase significantly but α did, which is not preferred; when silicon partially substituted yttrium and niobium and especially niobium, T_c increased significantly while α only increased mildly, which is desirable. When 3% of niobium was substituted by silicon, i.e., $\text{Fe}_{68.352}\text{B}_{23.04}\text{Y}_{4.608}\text{Nb}_1\text{Si}_3$, T_c reaches the maximum value of 296 °C and α remains a small value of $7.4 \times 10^{-6}/\text{K}$. This BMG has a high T_x of 648 °C, and as long as crystallization does not occur, the Invar effect stays. Comparing to the traditional Fe–Ni Invar alloy, this BMG has an inferior α , but has 115 °C higher T_c and about 9 times higher strength, exhibiting a potential for application as a new Invar material with moderate (low) thermal expansion, high operating temperature, and high strength.

11 September 2024, 07:45:28

ACKNOWLEDGMENTS

The authors acknowledge financial support from the National Natural Science Foundation of China (NSFC, No. 52061016) and fundings from the Jiangxi Academy of Sciences (Nos. 2021YBSBG21002, 2022YBSBG10001, and 2023YBSBG21013).

AUTHOR DECLARATIONS

Conflict of Interest

The authors have no conflicts to disclose.

Author Contributions

Z. R. Wang: Data curation (lead); Investigation (lead); Methodology (lead); Validation (lead); Writing – original draft (lead). **T. Yang:** Investigation (equal); Methodology (equal). **D. Wu:** Formal analysis (equal). **C. M. Wang:** Investigation (equal). **H. Guo:** Investigation (equal). **Q. Hu:** Conceptualization (lead); Funding acquisition (lead); Supervision (lead); Writing – original draft (equal); Writing – review & editing (equal). **S. Guo:** Writing – review & editing (equal).

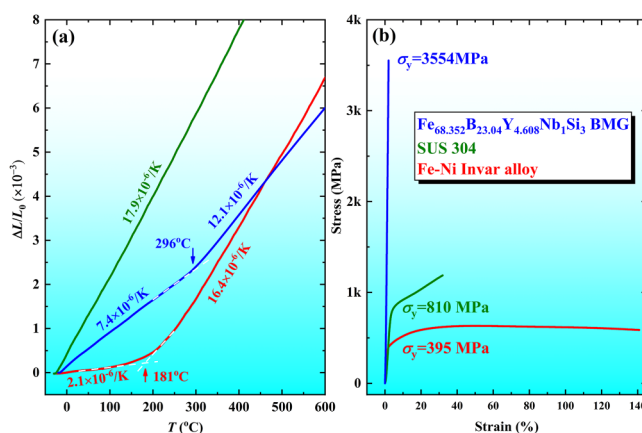


FIG. 11. (a) Thermal dilation traces and (b) compression stress–strain curves of three kinds of alloys.

DATA AVAILABILITY

The data that support the findings of this study are available from the corresponding author upon reasonable request.

REFERENCES

- ¹M. Shiga, *Curr. Opin. Solid State Mater. Sci.* **1**, 340 (1996).
- ²C. E. Guillaume, *Nature* **71**, 134 (1904).
- ³M. van Schilfgaarde, I. A. Abrikosov, and B. Johansson, *Nature* **400**, 46 (1999).
- ⁴Z. Rao, P.-Y. Tung, R. Xie, Y. Wei, H. Zhang, A. Ferrari, T. P. C. Klaver, F. Körmann, P. T. Sukumar, A. Kwiatkowski da Silva, Y. Chen, Z. Li, D. Ponge, J. Neugebauer, O. Gutfleisch, S. Bauer, and D. Raabe, *Science* **378**, 78 (2022).
- ⁵S. H. Lohaus, M. Heine, P. Guzman, C. M. Bernal-Choban, C. N. Saunders, G. Shen, O. Hellman, D. Broido, and B. Fultz, *Nat. Phys.* **19**, 1642 (2023).
- ⁶Y. Nakamura, in *Physics and Engineering Applications of Magnetism*, edited by Y. Ishikawa and N. Miura (Springer Berlin Heidelberg, Berlin, 1991), p. 111.
- ⁷A. Vinogradov, S. Hashimoto, and V. I. Kopylov, *Mater. Sci. Eng. A* **355**, 277 (2003).
- ⁸Q. Zhao, Y. Wu, J. He, Y. Yao, Z. Sun, and H. Peng, *J. Mater. Res. Technol.* **13**, 1012 (2021).
- ⁹Q. Hu, J. M. Wang, Y. H. Yan, S. Guo, S. S. Chen, D. P. Lu, J. Z. Zou, and X. R. Zeng, *Intermetallics* **93**, 318 (2018).
- ¹⁰C. Suryanarayana and A. Inoue, *Int. Mater. Rev.* **58**, 131 (2013).
- ¹¹H. X. Li, Z. C. Lu, S. L. Wang, Y. Wu, and Z. P. Lu, *Prog. Mater. Sci.* **103**, 235 (2019).
- ¹²J. Zhou, J. You, and K. Qiu, *J. Appl. Phys.* **132**, 040702 (2022).
- ¹³Q. Hu, X. R. Zeng, and M. W. Fu, *Appl. Phys. Lett.* **97**, 221907 (2010).
- ¹⁴D. H. Kim, J. M. Park, D. H. Kim, and W. T. Kim, *J. Mater. Res.* **22**, 471 (2011).
- ¹⁵P. Kamasa and P. Myslinski, *Cent. Eur. J. Phys.* **4**, 178 (2006).
- ¹⁶S. Ishio, M. Takahashi, Z. Xianyu, and Y. Ishikawa, *J. Magn. Magn. Mater.* **31–34**, 1491 (1983).
- ¹⁷Z. Xianyu, Y. Ishikawa, S. Ishio, and M. Takahashi, *J. Phys. F: Met. Phys.* **15**, 1787 (1985).
- ¹⁸S. Ishio and M. Takahashi, *J. Magn. Magn. Mater.* **50**, 93 (1985).
- ¹⁹Z. C. Lu, Z. Xianyu, B. G. Shen, and J. Liu, *Mater. Sci. Eng. A* **181**, 1001 (1994).
- ²⁰K. Narita, H. Fukunaga, and J. Yamasaki, *Jpn. J. Appl. Phys.* **16**, 2063 (1977).
- ²¹B. Huang, Y. Yang, A. D. Wang, Q. Wang, and C. T. Liu, *Intermetallics* **84**, 74 (2017).
- ²²A. Firlus, M. Stoica, G. B. M. Vaughan, R. E. Schäublin, and J. F. Löffler, *Mater. Today Nano* **24**, 100394 (2023).
- ²³A. Firlus, M. Stoica, S. Michalik, R. E. Schäublin, and J. F. Löffler, *Nat. Commun.* **13**, 1082 (2022).
- ²⁴V. Dolocan and E. Dolocan, *J. Magn. Magn. Mater.* **117**, 133 (1992).
- ²⁵N. Hassanain, H. Lassri, R. Krishnan, and A. Berrada, *J. Magn. Magn. Mater.* **146**, 37 (1995).
- ²⁶K. Fukamichi, M. Kikuchi, S. Arakawa, and T. Masumoto, *Solid State Commun.* **23**, 955 (1977).
- ²⁷A. Waske, B. Schwarz, N. Mattern, and J. Eckert, *J. Magn. Magn. Mater.* **329**, 101 (2013).
- ²⁸A. F. Manchón-Gordón, P. Svec, J. J. Ipus, M. Kowalczyk, J. S. Blázquez, C. F. Conde, A. Conde, P. Svec, and T. Kulik, *Metall. Mater. Trans. A* **51**, 1395 (2020).
- ²⁹E. A. Tereshina, D. I. Gorbunov, A. V. Andreev, and K. Watanabe, *IEEE Trans. Magn.* **47**, 3610 (2011).
- ³⁰W. Y. Yang, L. Zha, Y. F. Lai, G. Y. Qiao, H. L. Du, S. Q. Liu, C. S. Wang, J. Z. Han, Y. C. Yang, Y. L. Hou, J. B. Yang, X. Yu, and Z. Q. Qi, *Intermetallics* **99**, 8 (2018).
- ³¹A. Slawska-Waniewska and R. Zuberek, *J. Magn. Magn. Mater.* **160**, 253 (1996).
- ³²Z. Xianyu, Y. Ishikawa, S. Ishio, and M. Takahashi, *J. Magn. Magn. Mater.* **30**, 131 (1983).
- ³³M. Hatate, J. S. Garitaonandia, and K. Suzuki, *J. Appl. Phys.* **103**, 07E702 (2008).
- ³⁴H. J. Ma, J. T. Zhang, G. H. Li, W. X. Zhang, and W. M. Wang, *J. Alloys Compd.* **501**, 227 (2010).
- ³⁵J. M. Wang, Q. Hu, Y. H. Yan, and X. R. Zeng, *Chin. J. Mater. Res.* **32**, 691 (2018).
- ³⁶Q. Hu, X. R. Zeng, and M. W. Fu, *J. Appl. Phys.* **111**, 083523 (2012).
- ³⁷Z. C. Lu, Y. Z. Xian, B. G. Shen, and M. Q. Lv, *Acta Metall. Sin.* **30**, 265 (1994), <https://www.ams.org.cn/CN/Y1994/V30/I18/265>.
- ³⁸A. Van Den Beukel and S. Radelaar, *Acta Metall.* **31**, 419 (1983).
- ³⁹A. van den Beukel and J. Sietsma, *Acta Metall. Mater.* **38**, 383 (1990).
- ⁴⁰C. Nagel, K. Rätzke, E. Schmidtke, J. Wolff, U. Geyer, and F. Faupel, *Phys. Rev. B* **57**, 10224 (1998).
- ⁴¹Y. J. Huang, J. Shen, and J. F. Sun, *Appl. Phys. Lett.* **90**, 081919 (2007).
- ⁴²A. Slipenyuk and J. Eckert, *Scr. Mater.* **50**, 39 (2004).
- ⁴³X. R. Zeng, Q. Hu, M. W. Fu, and S. Xie, *J. Non-Cryst. Solids* **358**, 2682 (2012).
- ⁴⁴R. Brüning and K. Samwer, *Phys. Rev. B* **46**, 11318 (1992).
- ⁴⁵S. F. Guo, J. L. Qiu, P. Yu, S. H. Xie, and W. Chen, *Appl. Phys. Lett.* **105**, 161901 (2014).